

Curvature of point clouds through principal component analysis

Yasuhiko Asao* Yuichi Ike†

June 21, 2021

Abstract

In this article, we study curvature-like feature value of data sets in Euclidean spaces. First we formulate such curvature functions with desirable properties under the manifold hypothesis. Then we make a test property for the validity of the curvature function by the law of large numbers, and check it for the function we construct by numerical experiments. These experiments also suggest us to conjecture that mean of the curvature of sample manifolds coincides with the curvature of the mean manifold. Our construction is based on the dimension estimation by the principal component analysis and the Gaussian curvature of hypersurfaces. Our function depends on provisional parameters ε, δ , and we suggest to deal with the resulting functions as a function of these parameters to get some robustness. As an application, we propose a method to decompose data sets into some parts reflecting local structure. For this, we embed the data sets into higher dimensional Euclidean space by using curvature values and cluster them in the embedded space. We also give some computational experiments that support effectiveness of our methods.

Keywords: curvature, principal component analysis, manifold hypothesis, Gaussian random fields

1 Introduction

1.1 Motivation

Most of data we deal with often take the form of point clouds in Euclidean spaces. As many data analysts propose, they are often distributed around an embedded manifold in the Euclidean space, which is now called the *manifold hypothesis*. To extract some feature values from them is a pivotal task for data analysis. From the standpoint of the manifold hypothesis, estimating its curvature seems effective and natural. Several authors study the curvature of data from the view point of manifold learning or 3D shape study. See Subsection 1.4 for these related works.

In this article, we first formulate a curvature function of data to satisfy some desirable properties under the manifold hypothesis, and we construct a candidate

*Fukuoka University, 8-19-1 Nanakuma, Jonan-ku, Fukuoka city, Fukuoka, Japan.
asao@fukuoka-u.ac.jp

†Fujitsu Ltd., 4-1-1 Kamikodanaka, Nakahara-ku, Kawasaki, Kanagawa 211-8588, Japan.
yuichi.ike.1990@gmail.com, ike.yuichi@fujitsu.com

for such a function. Then we make a test property for the validity of the curvature function based on the law of large numbers, and check it for the function we construct. Our construction is based on the dimension estimation by the principal component analysis and the Gaussian curvature of hypersurfaces. We also give a computation algorithm for it as outlined in the next subsection.

1.2 Summary of our construction

Suppose that the data set X we deal with is a finite subset of the Euclidean space \mathbb{R}^n for some n . We estimate the curvature of X at $p \in X$ by the following procedure.

- (i) Fix thresholds $\varepsilon > 0, \delta > 0$.
- (ii) Calculate the eigenvalues $\lambda_1 \geq \dots \geq \lambda_n$ of the covariance matrix of the ε -neighborhood of p . Let u_1, \dots, u_n be the corresponding eigenvectors.
- (iii) Look at the eigenvalues $\lambda_1 \geq \dots \geq \lambda_K \geq \delta$ that are greater than the threshold δ . We regard the affine space $p + \langle u_1, \dots, u_K \rangle$ as the tangent space of the data at the point p , and also regard u_{K+1} as the normal direction at p .
- (iv) We give a frame and an orientation of the tangent space. We project all the points around p to the affine space spanned by the tangent space and the normal direction. Then we fit the resulting points by quadratic hypersurface in the affine space, and compute its Gaussian curvature at p with respect to the fixed frame.

The steps (i)–(iii) are essentially the same as principal component analysis. See Subsection 3.1 for the mathematical background of (i)–(iii), and see Proposition 3.2 for that of (iv). For the detail of the algorithm, see Section 4.

1.3 Contributions

Our contributions are the following.

- (1) In Section 2, we formulate curvature functions of data under the manifold hypothesis probability theoretically. Based on this formulation, we make a test property which is desirable for such a function. This property is verifiable by computations.
- (2) In Section 3, we define the “curvature” of point sets and give theoretical foundation that supports the validity of the definition. For that purpose, we investigate a modified version of principal component analysis and an estimation method of Gaussian curvature.
- (3) In Section 4, we propose a novel algorithm to compute the curvature based on the theoretical background. We also propose a clustering algorithm relying on the curvature values of a point set.
- (4) In Section 5, we experimentally show the effectiveness of our method using artificial and real-world data sets.

1.4 Related work

Our method first computes the tangent space at each point, which is related to studies in manifold learning (see, for example, [LV07, MF11, Wan12]). There one usually use k -nearest neighbor graph instead of a ball centered at each point as in our algorithm. Locally Linear Embedding (LLE) [RS00] estimates tangent spaces of a point set relying on k -nearest neighbor graph. [BM05] proposes a method to estimate tangent spaces by using neural networks whose input is global information of a point set, while LLE only uses local information. In most of the studies in manifold learning, it is often sufficient to estimate the tangent space for machine learning tasks, hence there are little studies on non-linear approximation of the manifold as in our method.

In 3D shape studies, curvature-like feature values have been studied from various point of views. [Tau95] proposes estimating curvature via polyhedral approximation. [LP05] computes curvature of a point set by solving some minimization problems to estimate tangent spaces. [CLS⁺19] studies the Weingarten map from a point set and estimates its convergence rate. In this article, we do not only focus on 3D shapes, but also explore a method that can be applied to broader type of data satisfying the manifold hypothesis.

A mathematical framework related to the manifold hypothesis is also given by [NSW08, NSW11]. In those paper, the authors consider Gaussian noise concentrated around a submanifold under the manifold hypothesis and discuss how to recover the homology from observations. There appears a quantity $1/\tau$ associated to an embedding of manifold that is deeply related to the curvature of the manifold. We have no idea about the relationship between $1/\tau$ and the curvature function we construct, and it is remained for our future work. In [AKTW18], they study the limit behavior of $1/\tau$ as the dimension of ambient space gets large. Subsequent research such as [FLR⁺14, CFL⁺17] studies the problem combining methods in topological data analysis with statistics. Our theoretical setting is somewhat similar to theirs (see Remark 2.1), but our method focuses on geometrical features rather than topological ones.

Acknowledgements

The first author was supported by RIKEN Center for Advanced Intelligence Project. The second author was partially supported by JST ACT-X (JPMJAX1903).

2 Framework

In this section, we explain the hypothetical framework under which we work.

Let Ω be a probability space. We consider a stochastic process $\Theta: \Omega \times \mathbb{R}^m \rightarrow \mathbb{R}^n$ centered at a manifold, that is, the restriction $\Theta(-, p): \Omega \rightarrow \mathbb{R}^n$ is measurable for every $p \in \mathbb{R}^m$, and the map $\int \Theta: \mathbb{R}^m \rightarrow \mathbb{R}^n$ defined by

$$\int \Theta(p) = \int \Theta(\omega, p) d\omega$$

is an embedding. We call such a stochastic process a *stochastic embedding*. We regard stochastic embeddings as a source of data obeying the manifold hypothesis.

We will later formulate data as some subset of the image of samples of stochastic embeddings.

Remark 2.1. If we have a restriction that $\Theta(\omega, p)$ varies (with respect to ω) only in the normal direction of the mean manifold at p , this formulation is very close to that of Niyogi–Smale–Weinberger’s [NSW11]. They consider that the distribution of data is induced from that on the normal bundle of a manifold. One of the merits of our approach using stochastic process is that we can deal with multiple points simultaneously which are generated with some noise from distinct points of the manifold. This is convenient to consider the curvature of the sample points. On the other hand, Niyogi–Smale–Weinberger consider a quantity $1/\tau$ associated to an embedded manifold that is a curvature-like quantity. However, it seems difficult to estimate $1/\tau$ from the data.

We denote by $\text{Emb}(\mathbb{R}^m, \mathbb{R}^n)$ the set of embeddings $\mathbb{R}^m \rightarrow \mathbb{R}^n$, and also denote by $\text{Emb}(\Omega \times \mathbb{R}^m, \mathbb{R}^n)$ the set of stochastic embeddings $\Omega \times \mathbb{R}^m \rightarrow \mathbb{R}^n$. We also denote by $\text{SP}(\Omega \times \mathbb{R}^m, \mathbb{R})$ the set of stochastic processes $\Omega \times \mathbb{R}^m \rightarrow \mathbb{R}$. Assume that we have a map $c: \text{Emb}(\mathbb{R}^m, \mathbb{R}^n) \rightarrow \text{Map}(\mathbb{R}^m, \mathbb{R})$ that extracts geometric feature of each point of embeddings, and we call such a map *curvature function*. For example, we can take c as the sectional curvature of the embedded manifold equipped with a metric induced from the standard metric of the ambient Euclidean space. We further assume that, corresponding to a curvature function c , there is a map $c_\Omega: \text{Emb}(\Omega \times \mathbb{R}^m, \mathbb{R}^n) \rightarrow \text{SP}(\Omega \times \mathbb{R}^m, \mathbb{R})$ that plays as a stochastic version of curvature function. We may expect that c_Ω is a ‘blurring’ of the curvature map c , and the expectation of c_Ω coincides with c . That is, the maps c and c_Ω are expected to satisfy the following commutative diagram:

$$\begin{array}{ccc} \text{Emb}(\Omega \times \mathbb{R}^m, \mathbb{R}^n) & \xrightarrow{c_\Omega} & \text{SP}(\Omega \times \mathbb{R}^m, \mathbb{R}) \\ \int \downarrow & & \downarrow \int \\ \text{Emb}(\mathbb{R}^m, \mathbb{R}^n) & \xrightarrow{c} & \text{Map}(\mathbb{R}^m, \mathbb{R}), \end{array} \quad (2.1)$$

where \int denotes the integration over Ω . We do not prove the existence of such a map c_Ω (it will be studied in our future work), but we can check it if we restrict $\text{Emb}(\Omega \times \mathbb{R}^m, \mathbb{R}^n)$ to the set of stochastic embeddings with the following conditions:

- (i) $m = 2, n = 3$, and $\int \Theta$ is a surface,
- (ii) $\Theta(\omega, -): \mathbb{R}^m \rightarrow \mathbb{R}^n$ is smooth for every $\omega \in \Omega$,
- (iii) $\partial_{ij}\Theta(-, p): \Omega \rightarrow \mathbb{R}^n$, the second derivatives at $p \in \mathbb{R}^m$, are uncorrelated for every p . That is, the covariance of each pair of the differentials is 0.

If Θ satisfies the above conditions, then the mean of the Gaussian curvature coincides with the Gaussian curvature of the mean manifold $\int \Theta$. We consider that such a restriction makes sense when we deal with the real-world data. For example, a Gaussian process $\Theta: \Omega \times \mathbb{R}^2 \rightarrow \mathbb{R}^3$ with $\Theta(\omega, p) = (p, t)$, $t \sim N(0, 1)$ whose covariance is determined the kernel $K(p, q) = p^T q$ satisfies the above. It is checked by calculating

$$\int \partial_{ij}\Theta(\omega, p)\partial_{i'j'}\Theta(\omega, p)d\omega = \partial_{ij}\partial_{i'j'}K(p, q)|_{p=q} = 0.$$

For another example, we can take the RBF kernel $K(p, q) = e^{-\|p-q\|}$ for the same process so that mean of the curvature coincides with the curvature of the mean. We can check it by calculating

$$\int \partial_{11}\Theta(\omega, p)\partial_{22}\Theta(\omega, p)d\omega = \partial_{11}\partial_{22}K(p, q)|_{p=q} = 4,$$

and

$$\int \partial_{12}\Theta(\omega, p)\partial_{12}\Theta(\omega, p)d\omega = \partial_{12}\partial_{12}K(p, q)|_{p=q} = 4.$$

We also check it numerically in Subsection 5.1.4.

Next we formulate the term “*data*” under the manifold hypothesis. Let X be a finite subset of \mathbb{R}^m . For a fixed $\omega \in \Omega$, we define a map $(\omega, X): \text{Emb}(\Omega \times \mathbb{R}^m, \mathbb{R}^n) \rightarrow \text{Map}(X, \mathbb{R}^n)$ by

$$(\omega, X)\Theta = \Theta(\omega, -)|_X.$$

We define a *data* as an element in $\text{Map}(X, \mathbb{R}^n)$ which is contained in the image of (ω, X) for some ω . For a data $D \in \text{Map}(X, \mathbb{R}^n)$, we call each element $D(x)$ for $x \in X$ a *datum*. We denote $\text{Data}_\Omega(X, \mathbb{R}^n)$ the set of data. A pivotal task of data analysis is to extract some feature value from a data which is a finite point cloud. Hence we formulate such task including curvature estimation as a map $\text{Data}_\Omega(X, \mathbb{R}^n) \rightarrow \text{Map}(X, \mathbb{R})$. In contrast to such maps, we regard c_Ω 's as ‘ideal feature value function’, and we expect that extraction from a data is an approximation of that by ideal function. Hence we define a *curvature function of data* $c_d: \text{Data}_\Omega(X, \mathbb{R}^n) \rightarrow \text{Map}(X, \mathbb{R})$ as a function with the following commutative diagram:

$$\begin{array}{ccc} \text{Emb}(\Omega \times \mathbb{R}^m, \mathbb{R}^n) & \xrightarrow{f \circ c_\Omega} & \text{Map}(\mathbb{R}^m, \mathbb{R}) \\ \downarrow X^* & & \downarrow X^* \\ \text{Map}(\Omega \times X, \mathbb{R}^n) & \xrightarrow{\tilde{c}_d} \text{Map}(\Omega, \text{Map}(X, \mathbb{R})) \xrightarrow{f} & \text{Map}(X, \mathbb{R}), \end{array}$$

where X^* denotes the restriction to X , \tilde{c}_d is only defined on $\text{Im}X^*$ by $\tilde{c}_d(X^*\Theta)(\omega) = c_d((\omega, X)\Theta)$, and the map f in the bottom is defined by $\int \varphi(x) = \int \varphi(x)(\omega)d\omega$ for any $\varphi \in \text{Map}(\Omega, \text{Map}(X, \mathbb{R}))$ and $x \in X$. If such a map c_d exists, then we have the convergence

$$\sum_i \frac{c_d(\omega) \circ X^*\Theta_i}{n} \rightarrow \int c_d(\omega)X^*\Theta_i d\omega = c|_X \int \Theta_i \quad (2.2)$$

Θ_i 's in $\text{Emb}(\Omega \times \mathbb{R}^m, \mathbb{R}^n)$ by the law of large numbers. In this article, we construct a candidate of the curvature function of data c_d and show its validity by checking (2.2) in Subsection 5.1.4.

3 Theoretical background

In this section, we give the theoretical background that supports our method. In the first subsection, we review *principal component analysis* with slight modification according to our usage. For the usual principal component analysis, we refer to, for example, [Jol86, AW10]. This subsection details the theoretical background of (i)–(iii) in Subsection 1.2. In the second subsection, we explain how to estimate curvature of point sets from Gaussian curvature of hypersurface by using principal components. This subsection details the background of (iv) in Subsection 1.2.

3.1 Our usage of principal component analysis

Let $X = \{p_1, \dots, p_N\} \subset \mathbb{R}^n$ be a finite subset and $p \in \mathbb{R}^n$. For an inner product space (W, \cdot) , we denote by $S(W)$ the set of all unit vectors in W . Let $u, v \in S(\mathbb{R}^n)$. We define *the covariance of X from p along u and v* by

$$V_X(p, u, v) := \frac{1}{N} \sum_{i=1}^N ((p - p_i) \cdot u) ((p - p_i) \cdot v).$$

We write $V_X(p, v, v) = V_X(p, v)$ and call it *the variance of X from p along v* . The variance $V_X(p, v)$ indicates how the data X is scattered in the direction v from the point p . We define *the covariance matrix of X from p* by $V_X(p) := (V_X(p, e_i, e_j))_{i,j} \in M_n(\mathbb{R})$, where e_i 's are the standard basis of \mathbb{R}^n . Using $V_X(p)$, we can write $V_X(p, v)$ as

$$\begin{aligned} V_X(p, v) &= \frac{1}{N} \sum_{i=1}^N ((p - p_i) \cdot v)^2 \\ &= \frac{1}{N} \sum_{i=1}^N v^T (p - p_i) (p - p_i)^T v \\ &= v^T \left(\frac{1}{N} \sum_{i=1}^N (p - p_i) (p - p_i)^T \right) v \\ &= v^T V_X(p) v. \end{aligned}$$

Hence all the eigenvalues of $V_X(p)$ are non-negative since $V_X(p, v) \geq 0$ for all v . The *principal component analysis* method gives an orthogonal decomposition $\mathbb{R}^n \cong W_1 \oplus \dots \oplus W_m$ such that any unit vector in $S(W_i)$ maximizes $V_X(p, v)$ under the restriction $v \in S(W_i \oplus \dots \oplus W_m)$. More precisely, we have the following proposition.

Proposition 3.1. *Let $\lambda_1 > \dots > \lambda_m$ ($1 \leq m \leq n$) be the eigenvalues of the covariance matrix $V_X(p)$, and let W_1, \dots, W_m be the corresponding eigenspaces, respectively. Then for $1 \leq i \leq m$ and any $v \in S(W_i)$,*

$$v = \operatorname{argmax}_{u \in S(W_i \oplus \dots \oplus W_m)} V_X(p, u).$$

Proof. For $u_i \in W_i$ and $v_j \in W_j$ with $i \neq j$, we have $u_i \cdot v_j = 0$ since $\lambda_i(u_i \cdot v_j) = u_i^T V_X(p) v_j = \lambda_j(u_i \cdot v_j)$. Hence W_i 's are orthogonal to each other. By

taking an orthonormal basis of each W_i 's, we have an orthonormal basis u_1, \dots, u_n of $W_1 \oplus \dots \oplus W_m$. We denote the eigenvalue corresponding to u_i by λ'_i . Obviously, we have $\lambda'_1 \geq \dots \geq \lambda'_n$. Let $v = \sum_{j=k}^n a_j u_j \in S(W_i \oplus \dots \oplus W_n)$. Since u_j 's are orthonormal, we have $\sum_{j=k}^n a_j^2 = 1$. Then we have

$$\begin{aligned} V_X(p, v) &= v^T V_X(p) v \\ &= \left(\sum_{j=k}^n a_j u_j \right)^T V_X(p) \left(\sum_{j=k}^n a_j u_j \right) \\ &= \left(\sum_{j=k}^n a_j u_j \right)^T \left(\sum_{j=k}^n \lambda'_j a_j u_j \right) \\ &= \sum_{j=k}^n \lambda'_j a_j^2 \leq \lambda'_k \leq \lambda_i. \end{aligned}$$

Hence, for any $v \in S(W_i \oplus \dots \oplus W_n)$, we obtain $V_X(p, v) \leq \lambda_i$. On the other hand, for $v \in S(W_i)$, we have $V_X(p, v) = v^T V_X(p) v = \lambda_i v^T v = \lambda_i$. This completes the proof. \square

Let us introduce a terminology for later use. Consider an embedding of a manifold $M \rightarrow \mathbb{R}^n$. If it factors through an embedding $\iota: M \rightarrow W$ for some affine subspace $W \subset \mathbb{R}^n$, we call the embedding ι an *efficient embedding*. From the standpoint of the manifold hypothesis that every point set we consider is distributed around an embedded manifold, the variance from a point on the manifold in the direction of its tangent vector should be large, while it should be very small in the other direction normal to the tangent space. Hence if we decompose \mathbb{R}_p^n , the set of all vectors from p , as $\mathbb{R}_p^n \cong W_1 \oplus \dots \oplus W_m$ by Proposition 3.1, it is reasonable to regard its subspace $W_1 \oplus \dots \oplus W_k$ as the tangent space at p . Here we fix some threshold $\delta > 0$, and k is determined by the conditions $\lambda_k \geq \delta$ and $\lambda_{k+1} < \delta$. By adding an eigenvector in W_{k+1} to this affine space, we regard it an ambient space in which the underlying manifold is efficiently embedded.

3.2 Estimation of Gaussian curvature

To estimate the curvature of a point set, we use the notion of Gaussian curvature of hypersurfaces. See [Pet06] for Gaussian curvature of Riemannian manifolds. It is known that if a hypersurface in \mathbb{R}^n is expressed by an explicit function as $x_n = f(x_1, \dots, x_{n-1})$ with $\partial f / \partial x_i = 0$ for $1 \leq i \leq n-1$, then its Gaussian curvature at the origin is expressed by the determinant of the Hessian $H_f = (\partial^2 f / \partial x_i \partial x_j)_{i,j}|_0$. If a manifold is efficiently embedded in codimension 1, then we can see the manifold as a hypersurface and compute its Gaussian curvature. Let $\iota: M \rightarrow \mathbb{R}^n$ be an embedding of d -manifold, and $a \in M$. Even if ι is not codimension 1, under the assumption that the linear space W spanned by the first and the second derivatives of ι at a is $(d+1)$ -dimensional, the following proposition guarantees that the orthogonal projection to W sufficiently approximates its Gaussian curvature at a by regarding the projected manifold as an embedding in W . Here we estimate the Gaussian curvature at a by

regarding the direction in W normal to the tangent space of $\iota(a)$ as the codimensional direction.

Proposition 3.2. *Let $\iota: \mathbb{R}^m \rightarrow \mathbb{R}^n$ be an embedding of class C^2 , and let $a \in \mathbb{R}^m$. Consider the \mathbb{R} -vector space W_a spanned by*

$$\left\{ \frac{\partial \iota}{\partial x_1}(a), \dots, \frac{\partial \iota}{\partial x_m}(a), \frac{\partial^2 \iota}{\partial x_1 \partial x_1}(a), \frac{\partial^2 \iota}{\partial x_1 \partial x_2}(a), \dots, \frac{\partial^2 \iota}{\partial x_m \partial x_m}(a) \right\}. \quad (3.1)$$

Then the affine space $\iota(a) + W_a \subset \mathbb{R}^n$ has the following property. Let $P: \mathbb{R}^n \rightarrow \mathbb{R}^n$ be the projection to $\iota(a) + W_a$. Then for any $\varepsilon > 0$, there exist $\varepsilon' > 0$ such that the map $\iota|_{B(a; \varepsilon')}$ is ε -close to $P \circ \iota|_{B(a; \varepsilon')}$ in C^2 , where $B(a; \varepsilon')$ denotes the ε' -ball centered at a .

Proof. We have $\iota|_{B(a; \varepsilon')}(a) = P \circ \iota|_{B(a; \varepsilon')}(a)$. Furthermore, since the affine space $\iota(a) + W_a$ is spanned by the vectors (3.1), we have

$$\begin{aligned} \frac{\partial}{\partial x_i} P \circ \iota(a) &= P \left(\frac{\partial \iota}{\partial x_i}(a) \right) = \frac{\partial \iota}{\partial x_i}(a), \\ \frac{\partial^2}{\partial x_i \partial x_j} P \circ \iota(a) &= P \left(\frac{\partial^2 \iota}{\partial x_i \partial x_j}(a) \right) = \frac{\partial^2 \iota}{\partial x_i \partial x_j}(a) \end{aligned}$$

for every $1 \leq i, j \leq m$. Hence the statement follows from the continuity of the map and the derivatives. \square

Now we provide our definition of “*curvature of embeddings and point sets*”, which is not the standard notion of curvature, but enough for extracting a feature value of embeddings or point sets. For an embedding ι , we choose a normal direction n_a of tangent space at $\iota(a)$ for each point $\iota(a)$, and denote by W_a the affine space spanned by the tangent space at $\iota(a)$ and n_a . We project the embedding ι to W_a and regard its image around $\iota(a)$ as a hypersurface in W_a . We define the curvature of the embedding at $\iota(a)$ as the Gaussian curvature at $\iota(a)$. By Proposition 3.2, this sufficiently approximates the Gaussian curvature in the situation explained right before the proposition. Let X be a point set and $p \in X$. If they are distributed around an embedding of a manifold, it is easy to understand the following, but our procedure is irrelevant to the assumption. As explained in Subsection 3.1, we regard the affine space $W_p = W_1 \oplus \dots \oplus W_k$ determined by some fixed $\delta > 0$ as the tangent space of the underlying manifold. We choose an eigenvector in W_{k+1} in the manner explained below, and regard it as the normal direction. We choose an orientation of the tangent space as explained later, and estimate the Gaussian curvature at p by fitting a polynomial surface around p regarded as a hypersurface. Note that, when the tangent space is even dimensional, the Gaussian curvature is independent of the choice of an orientation. It is checked by calculating the Hessian with respect to the orientation change. The choice of the normal direction and the orientation is done as follows. Let u_1, \dots, u_K be orthonormal basis of $W_p = W_1 \oplus \dots \oplus W_k$ such that each u_i belongs to some W_j . Such a basis exists since W_j 's are orthogonal to each other. See also the proof of Proposition 3.1. Consider u_i 's as points on the sphere S^{n-1} . We give a decomposition $U \sqcup S^{n-1} \setminus U$ such that $v \in U$ or $-v \in U$ for every point $v \in S^{n-1}$, then we choose u_i 's so that they belong to U . Let $S_+^{i-1} = \{(x_1, \dots, x_i) \in S^{i-1} \mid x_i > 0\}$ be the upper semi-sphere for $i \geq 0$.

Inductively we define $U_0 = \{1\} \subset S^0$ and $U_i = S_+^i \cup U_{i-1}$ for $1 \leq i \leq n-1$. Then the obtained $U_{n-1} \subset S^{n-1}$ satisfies the desired condition. We adjust the signatures of u_i 's so that they satisfy that $u_i \in U_{n-1}$. This determines a frame and an orientation of W_p , hence those of the tangent space at p . It also determines u_{K+1} , which is the normal direction.

4 Algorithm for computing curvatures of point clouds

In this section, we give our algorithm to compute the curvature of a given point set. We also provide a clustering algorithm of point sets depending on the curvature values. Until the end of this section, let X be a finite set in \mathbb{R}^n .

4.1 Curvature of point clouds

Our aim is to calculate a curvature-like quantity for each point $p \in X$. In order to work locally near $p \in X$, we fix a threshold $\varepsilon > 0$ and consider the subset $B := X \cap B(p; \varepsilon)$ of X , where $B(p; \varepsilon)$ denotes the open ball of radius ε centered at p . First we apply the principal component analysis described in Subsection 3.1 to B . That is, we diagonalize the covariance matrix $\text{Var}_B(p)$ as $U^T D U$, where $D = \text{diag}(\lambda_1, \dots, \lambda_n)$ with $\lambda_1 \geq \dots \geq \lambda_n$ and U is an orthogonal matrix. Write $U = [u_1, \dots, u_n]$. We give an orientation for u_1, \dots, u_n as in Subsection 3.2. It is pursued for each $u_i = (s_1^i, \dots, s_n^i)$ as follows. Look at the n -th coordinate s_n^i , and set $u_i = -u_i$ if $s_n^i < 0$, and remain if $s_n^i > 0$. If $s_n^i = 0$, look at the $(n-1)$ -th coordinate s_{n-1}^i and repeat this procedure.

Now, set another threshold $\delta > 0$ and let $\lambda_1 \geq \dots \geq \lambda_K \geq \delta$ be the eigenvalues at least δ . We consider the K -dimensional affine space $p + \langle u_1, \dots, u_K \rangle$ that is centered at p and spanned by vectors u_1, \dots, u_K . We regard K as the dimension of X around p , since the affine space would approximate the tangent space of the centered true manifold as explained in Section 3. The pseudocode for computing the dimension K and vectors u_1, \dots, u_K, u_{K+1} is shown in Algorithm 1.

Next, we shall compute the curvature of X at p . For a point $q \in \mathbb{R}^n$, we set $x_i(q) = (q - p) \cdot u_i$ for $i = 1, \dots, K+1$. We fit a quadratic hypersurface $x_{K+1} = \frac{1}{2} \sum_{i,j} a_{i,j} x_i x_j =: f(x_1, \dots, x_K)$ with $a_{i,j} = a_{j,i}$ to X . For this, we minimize the square error

$$E(a) = \sum_{q \in B} \left(\frac{1}{2} \sum_{i,j} a_{i,j} x_i(q) x_j(q) - x_{K+1}(q) \right)^2.$$

Solving the equations $\partial E / \partial a_{i,j} = 0$ gives $a_{i,j}$'s. We define the curvature of X at p by the Hessian H_f of f , which is computed as

$$H_f = \det \begin{bmatrix} a_{1,1} & \cdots & a_{1,K} \\ \vdots & \ddots & \vdots \\ a_{K,1} & \cdots & a_{K,K} \end{bmatrix}.$$

The pseudocode for computing the curvature is shown in Algorithm 2.

Combining the procedures described above, we obtain an algorithm to compute the dimension and the curvature of X at p given thresholds $\varepsilon, \delta > 0$. The pseudocode

for the overall algorithm is given in Algorithm 3. We can use the parameter ε as a persistent parameter as in topological data analysis, which encodes a multi-scale topological feature of a given point set. That is, varying ε from 0 to $+\infty$ we track change of values of dimension and curvature. A small ε reflects the local structure of P near p while a large reflects the global one. In Section 5, we show change of dimension and curvature depending on ε in various examples.

Algorithm 1: Compute dimension

input : X : point set, $p \in X$: point, ε, δ : positive numbers
output: $\dim(X, p; \varepsilon, \delta), (u_1, \dots, u_{\dim(X, p; \varepsilon, \delta)+1})$: non-negative integer and orthonormal vectors

- 1 COMPUTEDIMENSION($X, p; \varepsilon, \delta$)
- 2 $B \leftarrow X \cap B(p; \varepsilon)$;
- 3 $A \leftarrow \text{Var}_B(p)$;
- 4 diagonalize A as $U^T D U$ with $D = \text{diag}(\lambda_1, \dots, \lambda_n), \lambda_1 \geq \dots \geq \lambda_n$,
 $U = [u_1, \dots, u_n]$;
- 5 $K \leftarrow \#\{i \in \{1, \dots, n\} \mid \lambda_i \geq \delta\}$;
- 6 **return** $K, (u_1, \dots, u_{K+1})$

Algorithm 2: Compute curvature

input : B : point set, $p \in B$: point, u_1, \dots, u_K, u_{K+1} : orthonormal vectors
output: $\text{curv}(B, p; u_1, \dots, u_K, u_{K+1})$: real number

- 1 COMPUTECURVATURE($X, p; u_1, \dots, u_K, u_{K+1}$)
- 2 **foreach** $q \in B, i = 1, \dots, k + 1$ **do**
- 3 $x_i(q) \leftarrow (q - p) \cdot u_i$;
- 4 solve $\frac{\partial}{\partial a_{i,j}} \left(\sum_{q \in B} \left(\frac{1}{2} \sum_{i,j} a_{i,j} x_i(q) x_j(q) - x_{K+1}(q) \right)^2 \right) = 0$ with
 $a_{i,j} = a_{j,i}$;
- 5 **return** $\det \begin{bmatrix} a_{1,1} & \cdots & a_{1,K} \\ \vdots & \ddots & \vdots \\ a_{K,1} & \cdots & a_{K,K} \end{bmatrix}$

Algorithm 3: Compute dimension and curvature

input : X : point set, $p \in X$: point, ε, δ : positive numbers
output: $\dim(X, p; \varepsilon, \delta), \text{curv}(X, p; \varepsilon, \delta)$: non-negative integer and real number

- 1 COMPUTEDIMENSIONCURVATURE($X, p; \varepsilon, \delta$)
- 2 $K, (u_1, \dots, u_K, u_{K+1}) \leftarrow \text{COMPUTEDIMENSION}(X, p; \varepsilon, \delta)$;
- 3 $B \leftarrow X \cap B(p; \varepsilon)$;
- 4 $c \leftarrow \text{COMPUTECURVATURE}(B, p; u_1, \dots, u_K, u_{K+1})$;
- 5 **return** K, c

4.2 Clustering based on curvatures

Using the curvature values, we also propose a clustering algorithm. First we cluster the obtained curvature values, then add the cluster information as the fourth coordinate, and finally apply single-linkage clustering algorithm. More precisely, our clustering algorithm is the following:

- (i) set a scaling parameter $t > 0$ and a threshold $d, d' > 0$;
- (ii) compute the curvature value $c(p)$ for $p \in X$ depending on thresholds $\varepsilon, \delta > 0$ and set

$$a(p) := \begin{cases} -t & (c(p) < -d) \\ 0 & (|c(p)| \leq d) ; \\ t & (c(p) > d) \end{cases}$$

- (iii) embed X into \mathbb{R}^{n+1} by $p \mapsto (p, a(p))$ and write X' for the image;
- (iv) connect every two point in X' with distance less than d' by an edge and output the resultant connected components.

If we varies the threshold d' in the step (iv), this corresponds to computing 0-th persistence homology or hierarchical clustering. When we use a fixed threshold d' , one need to be set d' less than t so that the curvature coordinate effectively works. Namely, we want to distinguish two points p and $p + \varepsilon'$ that are very near but have quite different curvature value, hence the threshold should be smaller than $\lim_{\varepsilon' \rightarrow 0} d((p, 0), (p + \varepsilon', t)) = t$. In our experiments presented in Section 5, we set the distance threshold d' to be $t/2$. We remark that in the step (iv) we can use another method other than single-linkage clustering, such as k -means or mean-shift clustering. Applying a clustering algorithm to the embedded point set instead of the original X enables us to separate convex and concave parts in the point set. The experiment with artificial and real-world data sets will be shown in the next section.

Note also that single-linkage clustering algorithm corresponds to computing 0-homology. If we can output a point set providing a 1-homology class in the embedded point cloud in \mathbb{R}^4 by applying inverse analysis for homology class such as [EH16, Oba18], it would be helpful in practical applications. For example, we can distinguish two 1-cycles that are topologically homologous but are desired to be distinguished geometrically, such as cycles placed in a cylinder and a sphere which are tied by connected summation.

5 Experiments

In this section, we showcase our method to compute curvature-like quantity from artificial and real-world point sets. Although our method can be applied to point sets in any dimensional Euclidean space, we restrict ourselves to point sets in 3-dimensional space for visualization.

In practical use, the density around a point in a given point set X is different from point to point in general. Hence the number of point in the intersection $X \cap B(p; \varepsilon)$ heavily depends on a point p if we use a fixed ε . For this reason, we adjust ε for

each point, from the viewpoint of density. More precisely, for the radius of the ball centered at p we use $\varepsilon(p)$ computed as follows.

- (i) Fix a positive number $\eta > 0$ and set $r = 1/10 \times$ (the diameter of X).
- (ii) For $p \in X$, set $N(p) := \#(X \cap B(p; r))$, the number of points in $X \cap B(p; r)$.
- (iii) Define $\varepsilon(p) := 2\eta/N(p)$ for each $p \in X$.

In all the experiment in this section, we set η instead of ε . Moreover, the orientation was always taken as explained in Subsection 4.1.

5.1 Artificial data sets

In this subsection, we show the result of computation of the curvatures for artificial point sets.

5.1.1 Simple examples

First, we observe the behavior of our curvature value for two simple point sets. We generated two point sets consisting of 3000 points on the hypersurfaces $z = -x^2 - y^2$ and $z = x^2 - y^2$, respectively. The parameter ε was set as explained above with η equal to 3 times the diameter of the point set and $\delta = 0.001$. The results are shown in Figure 5.1.

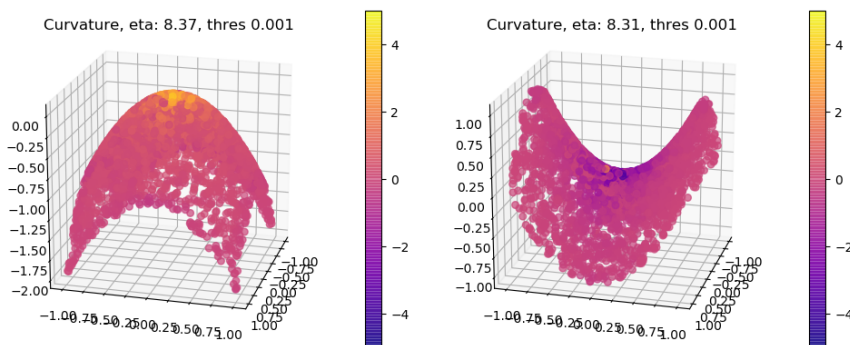


Figure 5.1: The curvature values for the surfaces $z = -x^2 - y^2$ and $z = x^2 - y^2$.

In these results, we can see that for the surface $z = -x^2 - y^2$ (left) the curvature values are positive while for $z = x^2 - y^2$ (right) the curvature values are negative, which coincide with the usual Gaussian curvatures $4/(1 + 4x^2 + 4y^2)^2$ and $-4/(1 + 4x^2 + 4y^2)^2$, respectively. As explained in Subsection 3.2, the curvature values are independent from the choice of frames since they are 2-dimensional.

5.1.2 Topologically similar examples distinguished by curvature values

Next we showcase two point sets that are difficult to distinguish by persistence homology but can be easily distinguished by our method. The point sets are displayed in the upper row of Figure 5.2. The first one is a finite set of 3000 points on the union of $S^1 \times [0, 1]$ and two discs (upper left), where we randomly sampled 1500

point from $S^1 \times [0, 1]$ and 750 points from discs, respectively. The second one is a finite set of 3000 points from the sphere with radius 0.5 (upper right). We computed the persistence homology of each point set and output the corresponding persistence diagram, which is shown in the middle row of Figure 5.2. Here, we used alpha complex for reducing the computation complexity, with the use of GUDHI library¹ in Python. We also computed the curvature values at each point in the point sets with $\eta = 3 \times$ (the diameter), $\delta = 0.001$ and made the histogram of the values, which is shown in the third row of Figure 5.2.

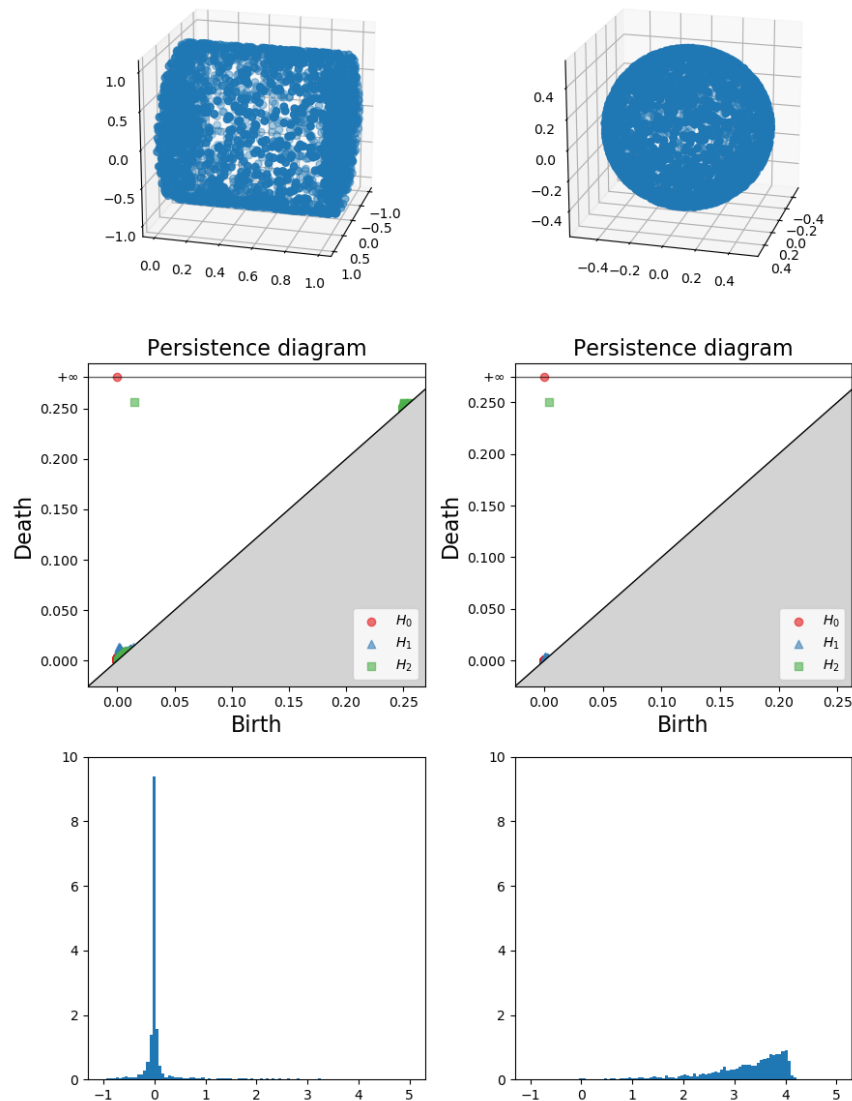


Figure 5.2: The two point sets that have similar persistence diagrams and different histograms of curvature values.

In these results, we can see the two point sets have similar persistence diagrams

¹<https://gudhi.inria.fr>

while they have very different histograms of curvature values. When the topological feature of data sets is not sufficient and more geometric information is needed for a task in question, our curvature values could be helpful in practical situation.

5.1.3 More examples of dimension and curvature estimation

Finally, we observe the behavior of curvature values depending on the choices of ε . For this purpose, we generated two artificial point sets as follows. The first one is the union of $S^1 \times [0, 1]$ and two discs same as in Figure 5.3 in Subsection 5.1.2. Here we randomly sample 1500 point from $S^1 \times [0, 1]$ and 750 points from each disc. The second one is a union of $S^1 \times [0, 1]$ and two hemi-ellipsoids (Figure 5.4). Similarly to the above, we randomly sample 1500 point from $S^1 \times [0, 1]$ and 750 points from each hemi-ellipsoid. We applied our algorithm to these point clouds consisting of 3000 points. Here the threshold δ was set to be 0.001 and where η was set to be

$$k \times (\text{the diameter of a given point cloud}) \quad (k = 1, 2, 3, 4). \quad (5.1)$$

The results are shown in Figures 5.3 and 5.4. The left columns show the estimated dimensions and the right ones indicate the curvatures.

We also applied our clustering algorithm explained in Subsection 4.2 to these point sets. We set the scaling parameter t to be 4, $d' = t/2$, and the threshold d to be 0.5. The results for clustering algorithm are showed in Figure 5.5 depending on different choices of ε . We can see that our clustering algorithm separates the convex and flat parts for each point sets.

5.1.4 Noisy datasets

In this subsection, we show the validity of our construction of curvature function by checking (2.2), that is, mean of the curvature coincides with the curvature of the mean manifold. We consider the behavior of our algorithm on noisy data.

We generate point sets by the following procedure. First, we generate randomly 1000 points a_1, \dots, a_{1000} on the plane \mathbb{R}^2 . Next, we consider a set of random variables (X_1, \dots, X_{1000}) that follows $N(0, C)$, the normal distribution with mean 0 and covariance matrix $C = (C_{ij})$ defined by

$$C_{ij} = \exp(-\|a_i - a_j\|_2^2).$$

Consider a surface $z = f(x, y)$ with $f \equiv 0$ or $f(x, y) = \pm\sqrt{1 - x^2 - y^2}$. We generate 1000 points by setting $p_i := f(a_i) + (\sigma X_i)n_i$, where $\sigma > 0$ and n_i is a unit normal vector of the surface at $f(a_i)$. The first distribution is same as the one explained in the fourth paragraph of Section 2. As mentioned in Remark 2.1, this modeling can also be seen as the model proposed by Niyogi–Smale–Weingberger [NSW11].

We compute the curvature values for the point set $X = \{p_1, \dots, p_{1000}\}$ for 50 times with $\sigma = 0.1, \eta = 1, \delta = 0.005$. Then we compute the mean of the curvature values for each i , which are displayed in Figure 5.6. We can see that mean of the curvature is very close to the curvature of the mean manifold.

Now we conjecture that for stochastic embeddings with suitable kernel function and suitable curvature function, the diagram (2.1) commutes. It has already verified for the distribution with $f(x, y) \equiv 0$ in the fourth paragraph of Section 2.

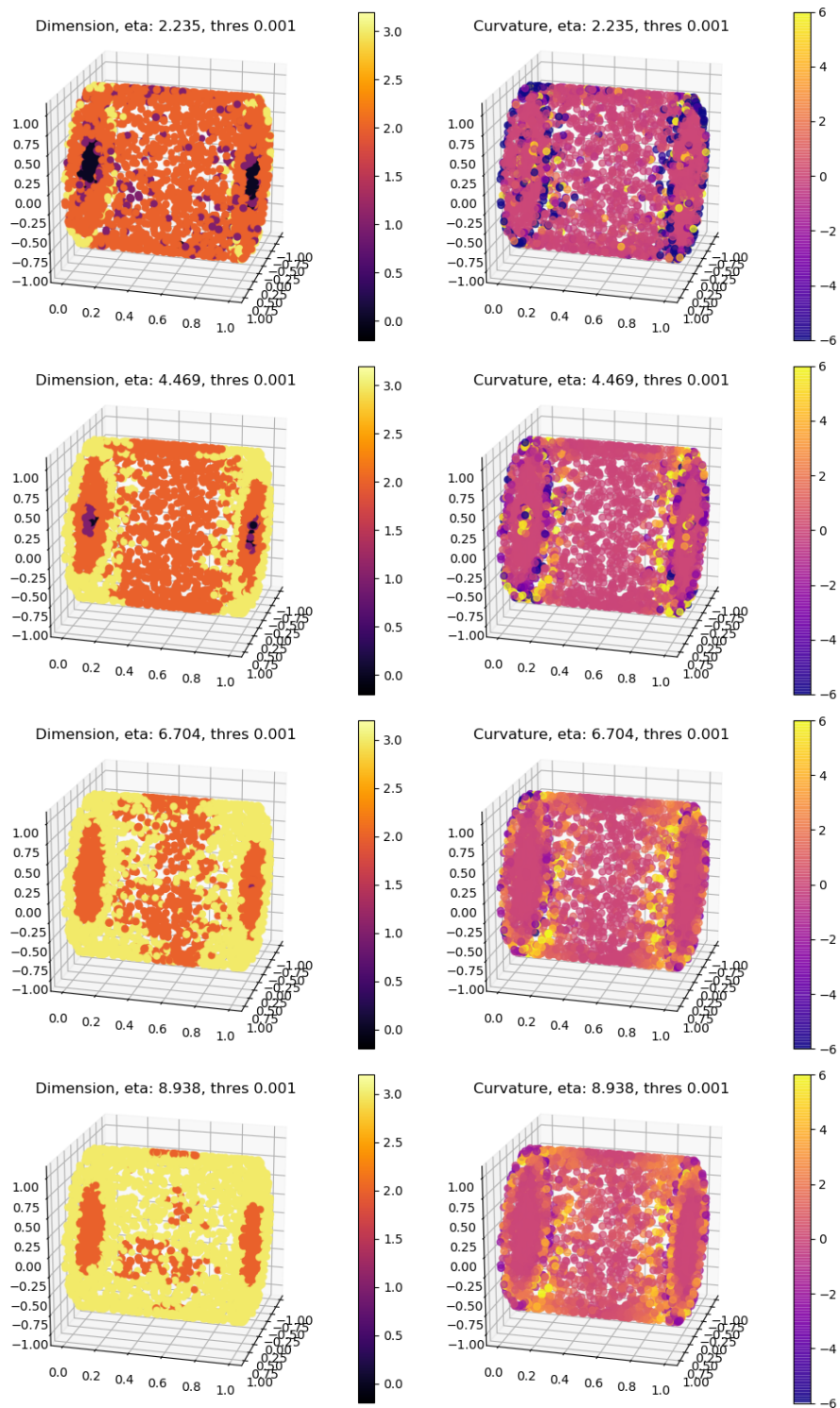


Figure 5.3: The estimated dimensions (left) and the curvature values (right) of $S^1 \times [0, 1]$ union two flat discs.

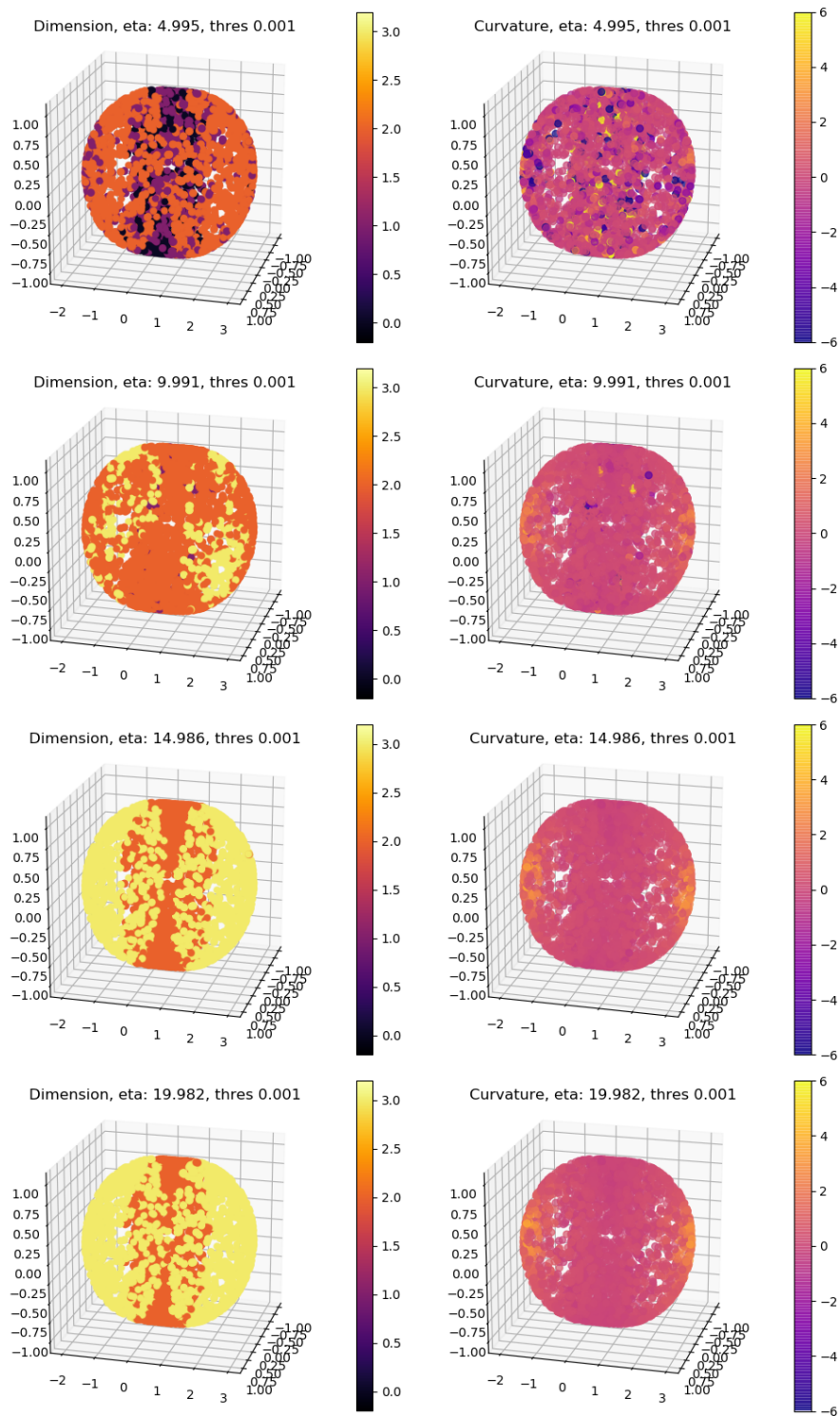


Figure 5.4: The estimated dimensions (left) and the curvature values (right) of $S^1 \times [0, 1]$ union two hemi-ellipsoids.

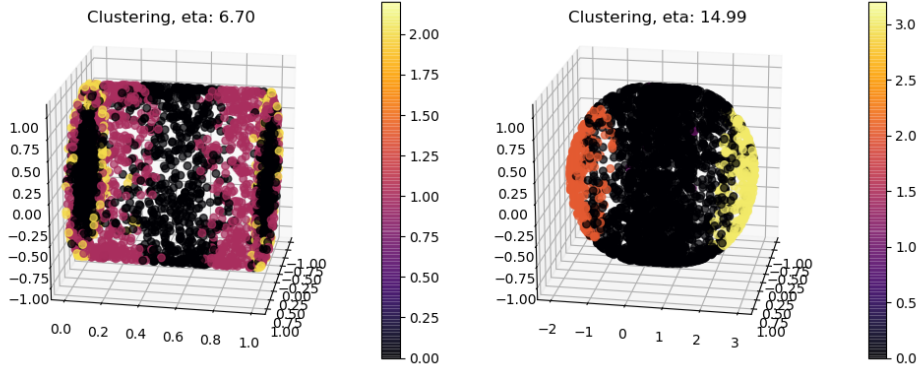


Figure 5.5: The clustering results of the artificial data sets.

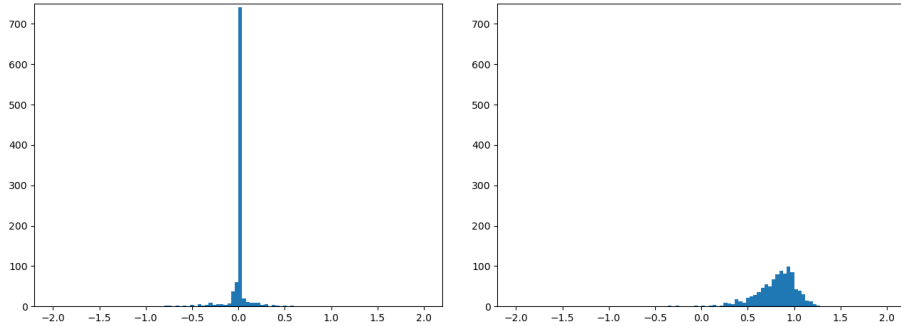


Figure 5.6: The distributions of the curvature values of noisy planes (left) and noisy spheres (right) with $\sigma = 0.1$. We generated point sets 50 times and computed the averages.

5.2 Real-world data sets

Now we show the results for real-world data sets. For these experiments, we used **G-PCD: Geometry Point Cloud Dataset**², from which we pick up Vase, Stanford Bunny, and Stanford Dragon point sets. We randomly took 3000 points from each point set and applied our algorithm, setting δ to be 0.001 and η varies as in (5.1). The results are shown in Figures 5.7 to 5.9.

In these results, we can find convex and concave parts in the point sets. Since we fit a quadratic surface to a point set locally in our method, the output curvature values may heavily change from point to point. Considering the curvature values for different ε would give some robustness.

Using the curvature values, we also applied the clustering algorithm presented in Subsection 4.2 to these point sets. Here, we set the scaling parameter t to be 4, $d' = t/2$, and the threshold d to be 0.5. The results are shown in Figure 5.10. We can see that our clustering method could distinguish convex and concave parts in the point sets.

²<https://www.epfl.ch/labs/mmspg/downloads/geometry-point-cloud-dataset/>

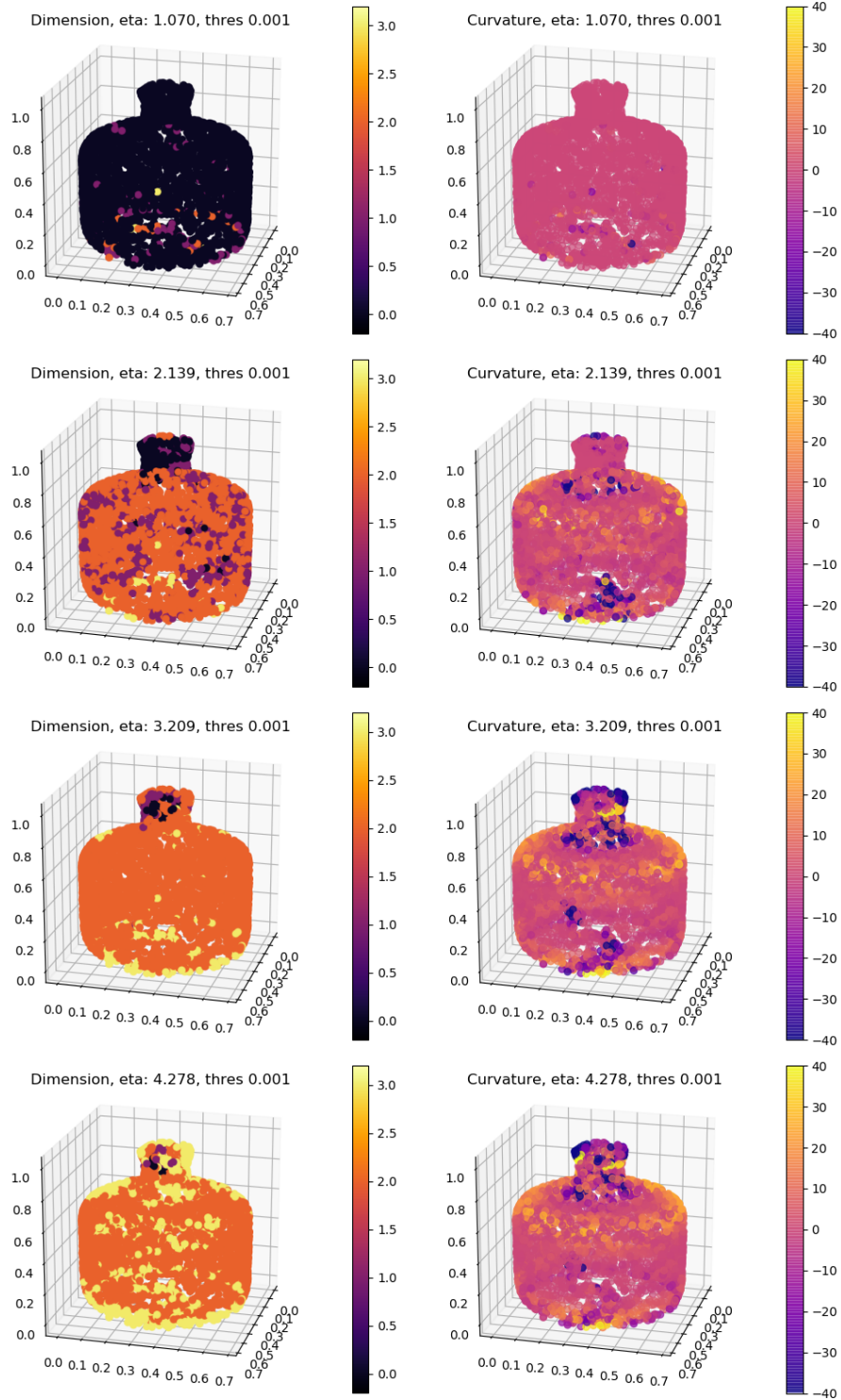


Figure 5.7: The estimated dimensions (left) and the curvature values (right) of the vase data set.

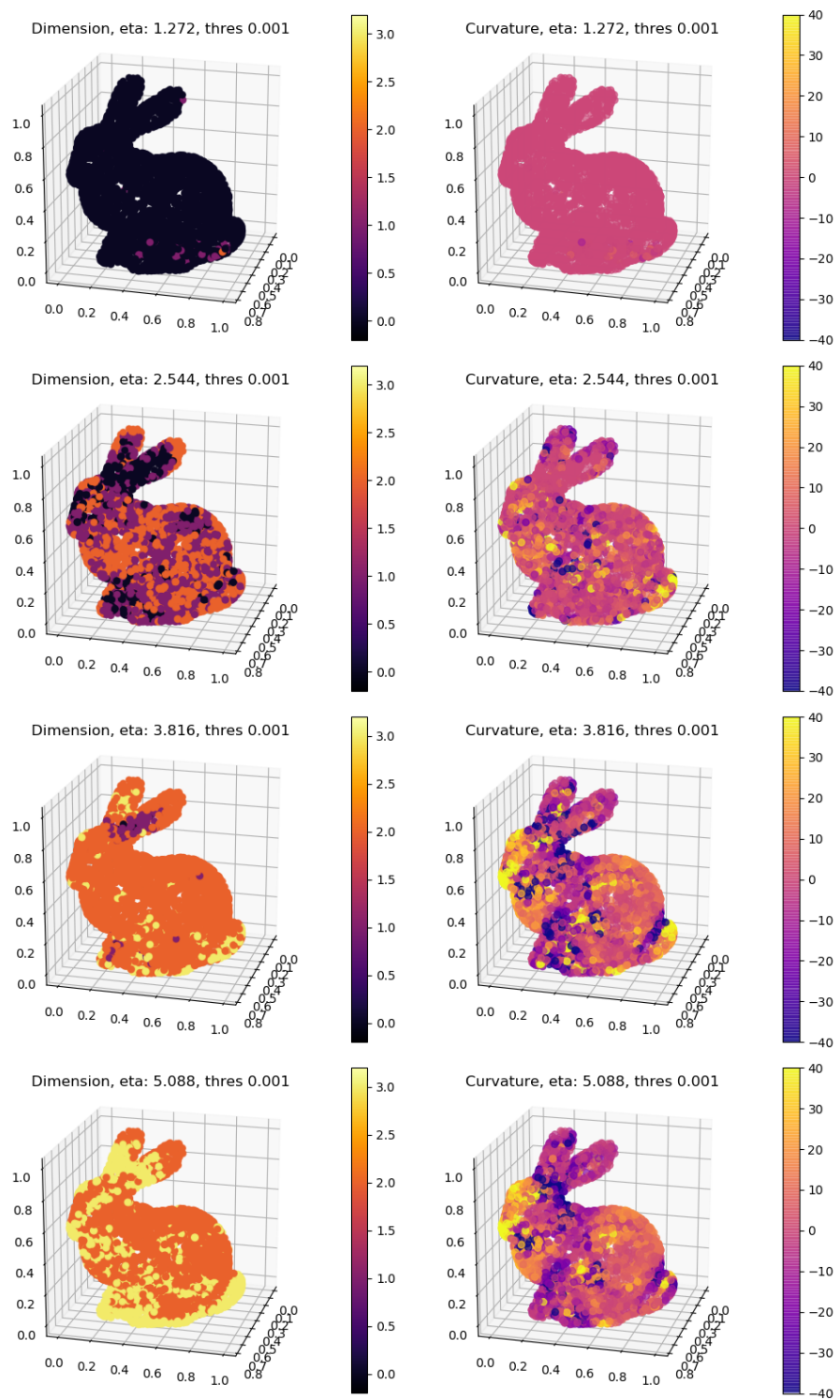


Figure 5.8: The estimated dimensions (left) and the curvature values (right) of the Stanford bunny data set.

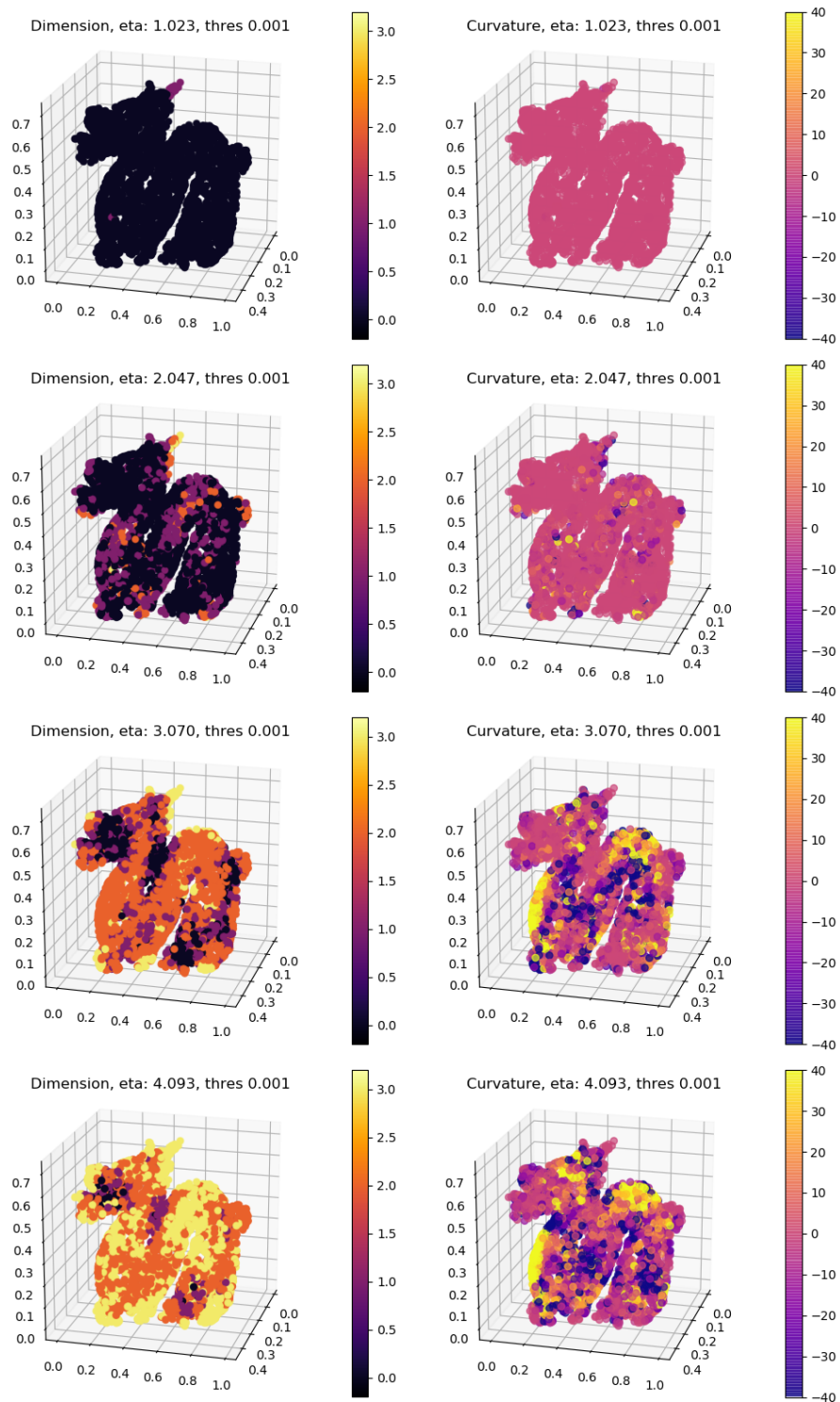


Figure 5.9: The estimated dimensions (left) and the curvature values (right) of the Stanford dragon data set.

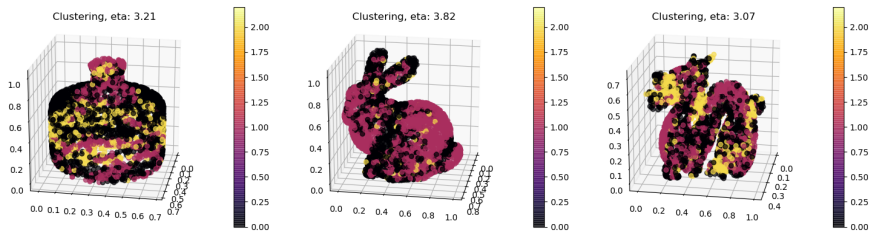


Figure 5.10: The clustering result of the real-world data sets.

6 Conclusion

Curvature is an essential quantity for studying spaces and would be helpful for studying point sets in data analysis. In this article, we have proposed a mathematical framework that indicates how the curvature of data should behave. Then we have given a construction of curvature function for data, and have shown its validity by numerical experiments. Here we conjecture that our framework is appropriate in the sense that the diagram (2.1) commutes in suitable situations. We also have proposed a method to compute the dimensions and the curvatures of point sets with respect to our definitions. We have also given some experimental results which support the effectiveness of our method. Fixing the parameter ε in our algorithm would take unexpected values due to noises, thus we proposed computing the curvature values as functions of ε . We expect that such function-like treatment would give robustness against noise, and we would build mathematical foundations for them in future work.

References

- [AKTW18] Robert J Adler, Sunder Ram Krishnan, Jonathan E. Taylor, and Shmuel Weinberger. Convergence of the reach for a sequence of gaussian-embedded manifolds. *Probability Theory and Related Fields*, 171(3):1045–1091, 2018.
- [AW10] Hervé Abdi and Lynne J Williams. Principal component analysis. *Wiley interdisciplinary reviews: computational statistics*, 2(4):433–459, 2010.
- [BM05] Yoshua Bengio and Martin Monoperrus. Non-local manifold tangent learning. In L. Saul, Y. Weiss, and L. Bottou, editors, *Advances in Neural Information Processing Systems*, volume 17. MIT Press, 2005.
- [CFL⁺17] Frédéric Chazal, Brittany Fasy, Fabrizio Lecci, Bertrand Michel, Alessandro Rinaldo, Alessandro Rinaldo, and Larry Wasserman. Robust topological inference: Distance to a measure and kernel distance. *The Journal of Machine Learning Research*, 18(1):5845–5884, 2017.
- [CLS⁺19] Yueqi Cao, Didong Li, Huafei Sun, Amir H Assadi, and Shiqiang Zhang. Efficient weingarten map and curvature estimation on manifolds. *arXiv e-prints*, arXiv:1905.10725 [stat.ML], 2019.

- [EH16] Emerson G Escolar and Yasuaki Hiraoka. Optimal cycles for persistent homology via linear programming. In *Optimization in the Real World*, pages 79–96. Springer, 2016.
- [FLR⁺14] Brittany Terese Fasy, Fabrizio Lecci, Alessandro Rinaldo, Larry Wasserman, Sivaraman Balakrishnan, Aarti Singh, et al. Confidence sets for persistence diagrams. *Annals of Statistics*, 42(6):2301–2339, 2014.
- [Jol86] Ian T Jolliffe. Principal components in regression analysis. In *Principal component analysis*, pages 129–155. Springer, 1986.
- [LP05] Carsten Lange and Konrad Polthier. Anisotropic smoothing of point sets. *Computer Aided Geometric Design*, 22(7):680–692, 2005.
- [LV07] John A Lee and Michel Verleysen. *Nonlinear dimensionality reduction*. Springer Science & Business Media, 2007.
- [MF11] Yunqian Ma and Yun Fu. *Manifold learning theory and applications*. CRC press, 2011.
- [NSW08] Partha Niyogi, Stephen Smale, and Shmuel Weinberger. Finding the homology of submanifolds with high confidence from random samples. *Discrete & Computational Geometry*, 39(1-3):419–441, 2008.
- [NSW11] Partha Niyogi, Stephen Smale, and Shmuel Weinberger. A topological view of unsupervised learning from noisy data. *SIAM Journal on Computing*, 40(3):646–663, 2011.
- [Oba18] Ipei Obayashi. Volume-optimal cycle: Tightest representative cycle of a generator in persistent homology. *SIAM Journal on Applied Algebra and Geometry*, 2(4):508–534, 2018.
- [Pet06] Peter Petersen. *Riemannian geometry*, volume 171. Springer, 2006.
- [RS00] Sam T Roweis and Lawrence K Saul. Nonlinear dimensionality reduction by locally linear embedding. *science*, 290(5500):2323–2326, 2000.
- [Tau95] Gabriel Taubin. Estimating the tensor of curvature of a surface from a polyhedral approximation. In *Proceedings of IEEE International Conference on Computer Vision*, pages 902–907. IEEE, 1995.
- [Wan12] Jianzhong Wang. *Geometric structure of high-dimensional data and dimensionality reduction*, volume 5. Springer, 2012.